Runout Tracking in Electric Motors Using Self-Mixing Interferometry

Reza Atashkhooei, Julio-César Urresty, Santiago Royo, Jordi-Roger Riba, *Member, IEEE*, and Luis Romeral, *Member, IEEE*

***Abstract*—In this paper, a self-mixing interferometry sensor has been used as a proximity probe to measure possible runout in permanent magnet synchronous motors, for fault diagnosis. A general procedure for the measurement of the 2-D trajectory of the motor shaft is described in detail, including procedures for the characterization of the uncertainty due to the shape of the shaft, and the management of speckle noise. The performance of the proposed sensor has been compared to that of a commercial Polytec laser vibrometer, for validation purposes. Results show inaccuracies in the order of ± 6 μm, which agree well with the measured uncertainty introduced by shaft surface imperfections.**

***Index Terms*—Feedback interferometry, motor shaft displacement, optical probe, permanent magnet synchronous motors (PMSMs), runout tracking, self-mixing, shaft proximity probe.**

I. Introduction

PERMANENT magnet synchronous motors (PMSMs) are becoming increasingly popular in high-performance applications, raising attention toward the corresponding condition monitoring and fault detection procedures. Static and dynamic misalignment of the motor shaft is a common origin of mechanical seal failure in PMSMs.

Several types of displacement or vibration sensors may be used as proximity probes to measure the shaft runout. The main families of sensors are eddy current probes, capacitive probes, linear variable differential transformer probes (LVDT), and laser Doppler velocimeters (LDV) [1]–[4]. Eddy current methods are practical, but the presence of metallurgical irregularities in the shaft can add high levels of noise in the results of the measurements, with the corresponding loss of accuracy [2]. Capacitive sensors are not limited by such an issue, but they need to be placed fairly close to the shaft (typically at distances of a few millimeters), which is not practical for *in situ* measurements. LVDT probes are contact methods limited in its sensing speed by the inertia of the moving tip, which in addition is subjected to wear and warm up, and to damage by surface irregularities. As a noncontact technique operative at a distance from the shaft, LDV avoids all these inconveniences, but it may suffer from speckle noise and is a quite expensive equipment [5].

In this paper, we propose a self-mixing interferometry (SMI) probe, which is a particular arrangement of laser vibrometry [6] specially suited to harsh measurement conditions. The self-mixing phenomenon has been studied in depth in the last decades and shown to perform nicely as a noninvasive sensor for displacement, vibration, distance, and velocity measurements [7]–[10].

In SMI we take an advantage of the portion of the emitted beam from the laser diode (LD), which is back-reflected from the target and re-enters the laser cavity, getting self-mixed with the original beam. As a consequence, a variation of the spectral properties of the laser beam and its emitted optical intensity is introduced.

The output optical power (OOP) of the LD may be monitored using the photodiode (PD) typically integrated in the same laser package, making the interferometer extremely compact and self-aligned. When the target moves, the optical path length changes causing sawtooth-like variations in the OOP. It can be shown that every peak in the OOP corresponds to a $\lambda/2$ displacement of the target, where λ is the wavelength of the laser, becoming equivalent to a fringe in an interferogram [11]. The compactness, simplicity, and cost effectiveness of the sensor, together with its noncontact nature, make it a very suitable solution to track runout in electrical motors, with measurement accuracies below half the wavelength of the laser.

The rest of this paper is organized as follows. The measurement method proposed, including the measurement principle, procedure, and the estimation of the uncertainty due to the surface imperfections in the motor shaft will be explained in Section II. In Section III, the results of the self-mixing sensor for runout measurement will be validated by comparison with the results of a commercial LDV.

Measurement results for 2-D runout in a PMSM are presented in Section IV, both for a healthy and a faulty motor, showing the potential of the technique for motor testing purposes.

II. Measurement Method

A. Measurement Principle

The theoretical model of SMI is now well known and described by the Lang and Kobayashi equations [12]. The modified

Manuscript received June 2, 2012; revised September 19, 2012; accepted October 7, 2012. Date of publication November 26, 2012; date of current version January 17, 2014. Recommended by Technical Editor R. Moheimani. This work was supported in part by the Spanish Ministry for Science and Innovation under the DPI2011-25525 research project and in part by the Technical University of Catalonia under an FPI-UPC Grant.

R. Atashkhooei and S. Royo are with the Center for Sensors, Instruments, and Systems Development (CD6 Research Center), Universitat Politècnica de Catalunya, Terrassa 08222, Barcelona, Spain (e-mail: reza.atashkhooei@cd6.upc.edu; santiago.royo@upc.edu).

J.-C. Urresty and L. Romeral are with the Department of Electronic Engineering, Universitat Politècnica de Catalunya, Terrassa 08222, Barcelona, Spain (e-mail: julio.urresty@mcia.upc.edu; romeral@eel.upc.edu).

J.-R. Riba is with the Department of Electrical Engineering, Universitat Politècnica de Catalunya, Terrassa 08222, Barcelona, Spain (e-mail: riba@ee.upc.edu).

Color versions of one or more of the figures in this paper are available online at http://ieeexplore.ieee.org.

Digital Object Identifier 10.1109/TMECH.2012.2226739

phase of the emitted light in the presence of feedback is given by

$$\phi_F(t) = \phi_0(t) - C \,.\, \sin\left[\phi_F(t) + \arctan(\alpha)\right] \tag{1}$$

where α is a parameter of the LD called the linewidth enhancement factor, C is the feedback coupling factor representing the external feedback strength, and $\phi_F(t)$ and $\phi_0(t)$ are the signal phases with and without feedback, respectively, given by

$$\phi_F(t) = 2\pi \frac{D(t)}{\lambda_F(t)/2} = 4\pi\nu_F(t)D(t)/c \tag{2}$$

$$\phi_0(t) = 2\pi \frac{D(t)}{\lambda_0(t)/2} = 4\pi\nu_0(t)D(t)/c \tag{3}$$

where $\lambda_F(t)$ and $\lambda_0(t)$ are the LD wavelengths with and without feedback, $D(t)$ is the distance from the LD to the target, and c is the speed of light. $\nu_F(t)$ and $\nu_0(t)$ are the optical frequencies of the LD with and without feedback, respectively. The phase of the signal under feedback can be related to the OOP of the LD under feedback, which is obtained as [13]

$$P_F(t) = P_0(1 + m \,.\, \cos(\phi_F(t)) \tag{4}$$

where P_0 is the OOP of the LD without feedback and m is the modulation index (typically $m = 10^{-3}$). The phase signal under feedback can be extracted from the OOP using a simple fringe counting algorithm [14], [15], yielding a displacement measurement with a basic resolution of $\lambda/2$. Different approaches have been proposed to improve the resolution of the technique, such as the phase-unwrapping [15] or the slope-based methods [16], which allow displacement measurements with accuracies below $\lambda/16$. However, in the present application the basic resolution of the SMI sensor is far below the uncertainty of the measurement introduced by the experimental setup (see Section II-C), so the fringe counting method will be used in the measurements as a phase reconstruction algorithm.

In practical applications under industrial conditions, like the ones in which we intend to use the sensor, a number of parasitic phenomena are present, especially when large motors are involved. These phenomena include mechanical coupling, electromagnetic disturbances, or surface imperfections of the target, among others. These phenomena may introduce noise into the OOP of the LD, as white-like noise or sparkle-like noise out of electromagnetic or mechanical sources in the environment. In addition, using a laser source may introduce speckle noise [8] due to coherent superposition of the laser light randomly scattered from the target surface. When the displacement range in which the self-mixing signal (SMS) amplitude is modulated becomes large, it is likely to find dark speckle regions where the amplitude of the SMS is faded to the noise level. In these regions, some fringes may be hidden by noise and left undetected, leading to inaccurate displacement reconstruction.

Some signal preprocessing solutions have been proposed to efficiently remove the white-like and sparkle-like noise and improve the signal-to-noise ratio (SNR) such as low-pass averaging filter [17], Kaiser-based FIR filter after a median filter [18], adaptive digital filters [19], or neural network interpolation [20].

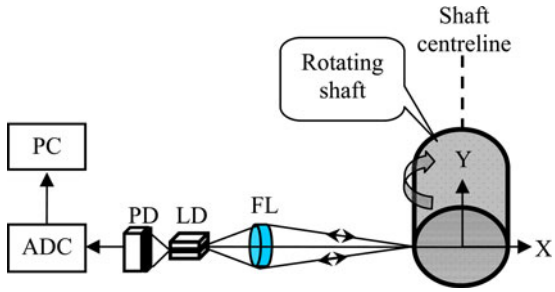

Fig. 1. Schematic diagram of the experimental configuration.

For our purposes, a simple low-pass averaging filter was enough to remove the high-frequency component of noise present in the signal (see Section II-B for more details).

A number of solutions have also been proposed to overcome the speckle noise problem [8], such as speckle tracking [21], where a piezoelectric positioning system is used to move the laser beam in perpendicular to the optical axis while looking for an intense speckle spot to keep the signal amplitude at the maximum possible level. Alternative approaches have used an adaptive technique based on a liquid lens [22], [23], which has been shown to actively modify the laser beam spot size and feedback strength to keep the signal amplitude at the proper level. The use of a double LD solution [23], which combines the signals of two LDs with different beam spot sizes on the target has also been proposed.

Since the shaft runout is moving at high speed and the measurement should be taken in a single point adjusted perpendicular to the expected symmetry axis of the shaft, the double LD solution which uses two lasers pointing to different points on the shaft cannot be used, because we need to monitor the vibration at a single point of the shaft. Similarly, the described speckle tracking technique introduces an in-plane displacement of the optical axis which does not modify the aperture of the beam and, in addition, introduces a random misalignment component in the measured signal. For this reason, we used a version of the adaptive solution described before by adjusting the focus position of the focusing lens (FL) through the manual displacement of the lens along its optical axis, prior to the measurement, in order to experimentally minimize the amplitude of the speckle noise.

B. Measurement Procedure

Since the shaft displacement is the measurement subject, the laser diode has been arranged to point in perpendicular to the shaft centerline using an FL, as depicted in Fig. 1. The OOP monitored by the PD integrated in the laser package is saved in the PC after an analog-to-digital conversion (ADC). The vibration of the shaft in the laser beam direction (see the X-axis in Fig. 1) is measured by offline signal processing. All measurements were performed using a Hitachi HL7851G self-mixing LD (SMLD) emitting at 785 nm with a maximum output power of 50 mW.

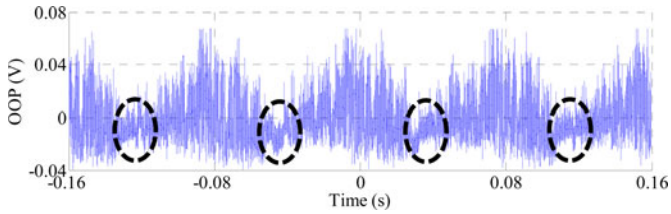

Fig. 2. Speckle affected SMS generated by rotating shaft displacement. Four rotations at 12.5 Hz are plotted.

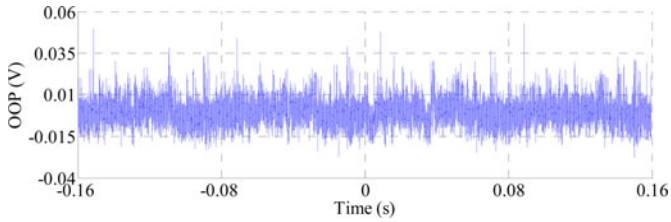

Fig. 3. SMS generated by rotating shaft displacement after focus compensation. Four rotations at the frequency of 12.5 Hz.

The motor used for the tests was a PMSM with reference no. ABB:8C1360, maximum power of 2.5 kW, and maximum rotation frequency of 33.3 Hz. In the measurements rotation, frequencies were set to 12.5 and 25 Hz, to test the motor under typical operating conditions.

Due to the system configuration, speckle noise resulting in broad-scale SMS amplitude modulation has been observed. Fig. 2 shows the acquired SMS generated by the displacement of a typical PMSM shaft after four complete turns.

It may be observed how the acquired SMS includes one periodic black-out zone at each rotation (marked with dashed circles) where the signal amplitude reaches the noise level, leading to a poor SNR and inaccurate reconstruction.

As the average speckle size depends on the target distance from the LD and the beam aperture at the entrance pupil of the lens [8], [24], the speckle pattern can be modified by changing the position of the beam focus along the optical axis (by manually adjusting the position of FL prior to the measurement), in order to keep the SMS amplitude above the threshold of signal loss along the whole acquisition period, and also to get the minimum possible modulation frequency. Obviously, during the shaft rotation, the speckle pattern is almost repeated for each rotation as seen in Fig. 2. By changing the focus position of FL, and observing the signal at the oscilloscope screen, the best focus position to get minimally modulated signal amplitude is found. The future implementation of an automated FL adjustment or the use of a voltage programmable liquid lens [22] will result in autonomous performance of the sensor. Using this new procedure leads to adequate SNR values in the whole signal removing the amplitude fading effect introduced by speckle modulation, enabling proper displacement reconstruction.

Fig. 3 shows the acquired SMS once spot size has been optimized, with no black-out zones present. The whole scheme of signal processing for the SMS obtained is presented in Fig. 4, showing the four processing steps involved.

As a first step, a low-pass Butterworth-type filter is applied to the SMS to clean it from unwanted high-frequency noise. The cutoff frequency of the filter was fixed to 15% of the sampling frequency.

In a second step, the modified signal phase $\phi_F(t)$ is estimated as in [15]. As the modified phase is related to the OOP by (4), after an automatic gain control algorithm which normalizes the signal to ± 1, the arcos function is applied to obtain the value of $\phi_F(t)$ modulus π. Afterward, to properly unwrap the phase, the derivative of $\phi_F(t)$ is calculated and thresholded to detect the position of the fringes, and normalized to ± 1. Finally, an integrator algorithm adds or subtracts the phase jumps ($\approx 2\pi$) at the detected fringe positions. Finally, the value of displacement related to the phase $\phi_F(t)$ by (2) can be obtained by multiplying $\lambda/4\pi$ to $\phi_F(t)$.

An additional compensation algorithm has been introduced to account for the misalignment error introduced if the LD is not pointing perpendicularly to the shaft surface with half-wavelength accuracy. This processing step is specially implemented for the current application as a new additional algorithm. In case this misalignment error is present, virtual displacements of the shaft will appear in the reconstructed signal, caused by the component of the velocity of the surface in the direction of the beam (see Fig. 5). This error is hardly avoidable in practice, so this component of the displacement is eliminated as the last step of the signal processing procedure, by estimating the average speed and removing the introduced virtual displacement.

Fig. 6 shows the experimental results of the reconstructed displacement after four rotations of the shaft at a frequency of 12.5 Hz. The component in the direction of the laser beam introduces a constant speed component on the measured periodic displacement.

Fig. 7 shows the reconstructed displacement after removing the unwanted component of the displacement leading to maximum peak-to-peak amplitudes of about 52.9 μm.

C. Uncertainty Estimation

There is an additional source of uncertainty in the measurement of displacement due to the mechanical imperfections of the rotor shaft surface such as roundness errors, scratches, material irregularities, shape errors, or other causes of eccentricity of the shaft, which are randomly added to the measurement. These imperfections bring on a level of uncertainty in the measurement, which prevents from reaching the half-wavelength resolution of the measurement technique.

To evaluate the level of uncertainty introduced by this effect, a new approach including two SMLDs was collinearly aligned at both sides of the shaft, as shown in Fig. 8. The displacement of one of the SMLDs relative to the other in the absence of mechanical imperfections is expected to be linear, with only a constant phase delay in the absolute signals, in the absence of errors. Variations from this linearity should be considered as an effect of mechanical imperfections.

Fig. 9 shows the experimental results for this uncertainty estimation. Using the setup of Fig. 8, the SMS was acquired for four rotations of the shaft at 12.5 Hz.

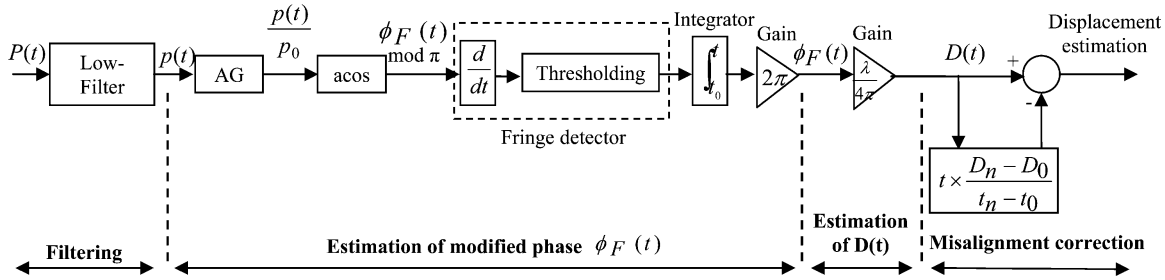

Fig. 4. Signal processing block diagram for estimation of the displacement, including misalignment correction.

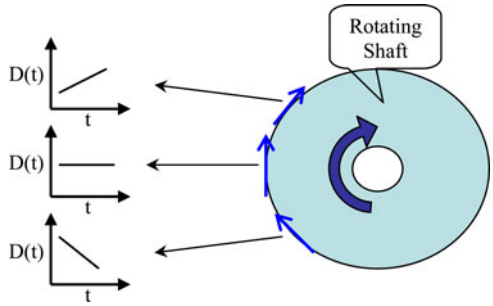

Fig. 5. Displacements due to the misalignment of LD beam position on shaft surface.

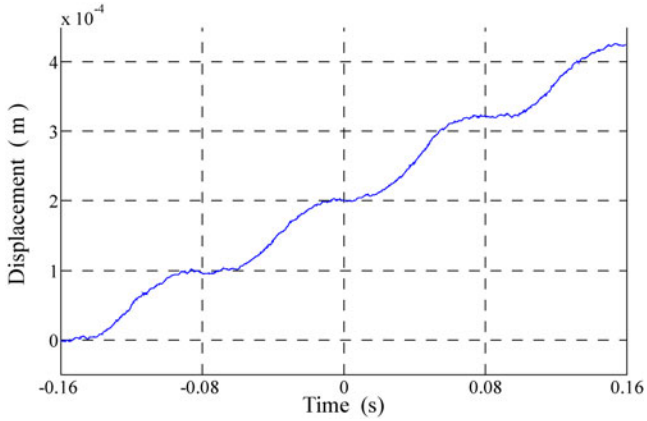

Fig. 6. Reconstructed displacement of the rotating shaft for four rotations at the frequency of 12.5 Hz.

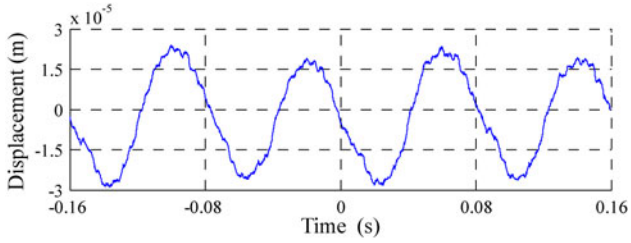

Fig. 7. Reconstructed displacement for four rotations at the frequency of 12.5 Hz after the removal of the unwanted displacement due to the misalignment.

The uncertainty obtained in the displacement reconstruction was below ± 6 μm, corresponding to $\pm 11.3\%$ of the total displacement range measured.

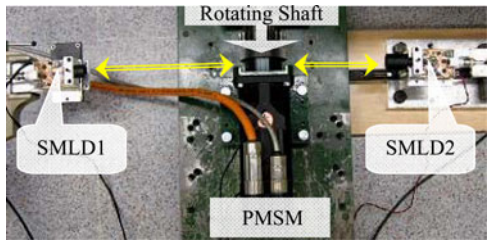

Fig. 8. Two LD configuration to estimate the uncertainty of the measurements.

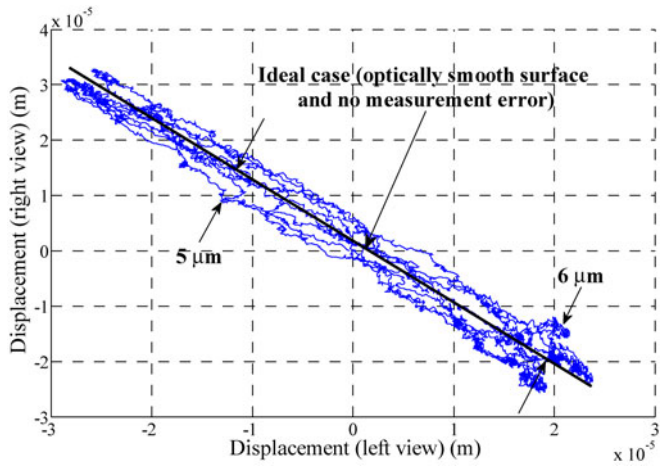

Fig. 9. Reconstructed displacement from the left view (obtained by SMLD1) against the reconstructed displacement from the right view (obtained by SMLD2) for four rotations with the frequency of 12.5 Hz.

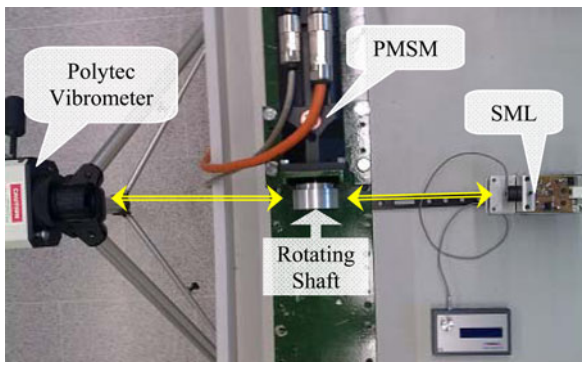

Fig. 10. Experimental configuration for shaft runout measurement using two laser vibrometers for comparison purpose.

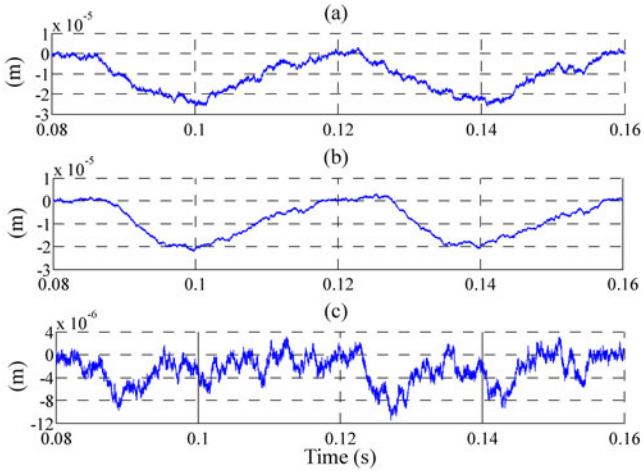

Fig. 11. Signal reconstructions of a typical PMSM shaft displacement at horizontal direction using polytec vibrometer and an SMLD for two rotations with the frequency of 25 Hz. The difference is the subtraction of two reconstructed signals. (a) Displacement (by SMLD). (b) Displacement (by Polytec Vibrometer). (c) Difference (between displacements).

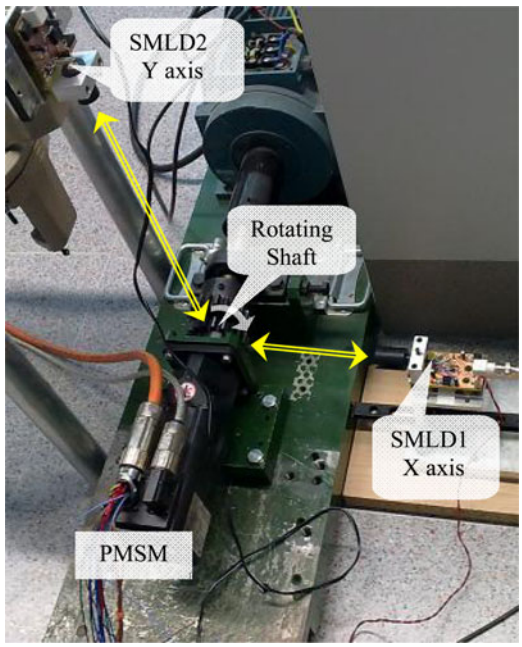

Fig. 12. 2-D measurement configuration for motor shaft runout tracking.

III. Measurement Validation

To validate the measurements obtained using the proposed technique, a commercial Polytec OFV-303 laser vibrometer has been used. Fig. 10 shows the experimental setup, with the Polytec vibrometer pointing to one side of the shaft centerline and the SMLD pointing to the opposite side, collinearly and at the same height.

The goal is to measure the lateral displacement of the shaft centerline by both vibrometers at the same position, comparing them once the difference in displacement direction has been compensated.

Fig. 11 shows the reconstructed signals of both vibrometers for lateral displacement of the rotating shaft of a typical PMSM.

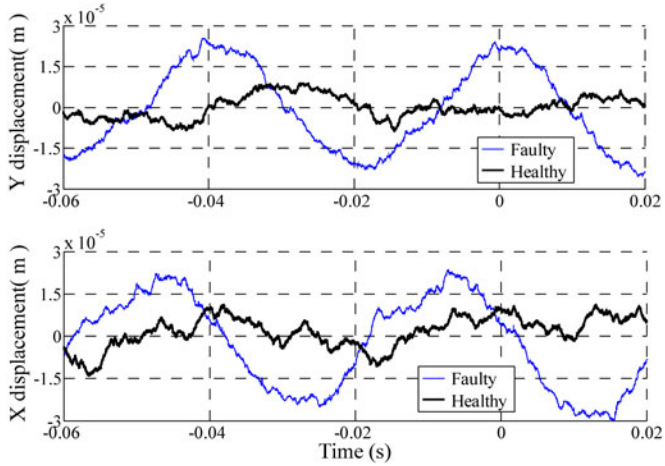

Fig. 13. Reconstructed shaft displacements in the X- and Y-axes for a healthy and a faulty PMSM when running at 25 Hz. Two periods are acquired in the measurement.

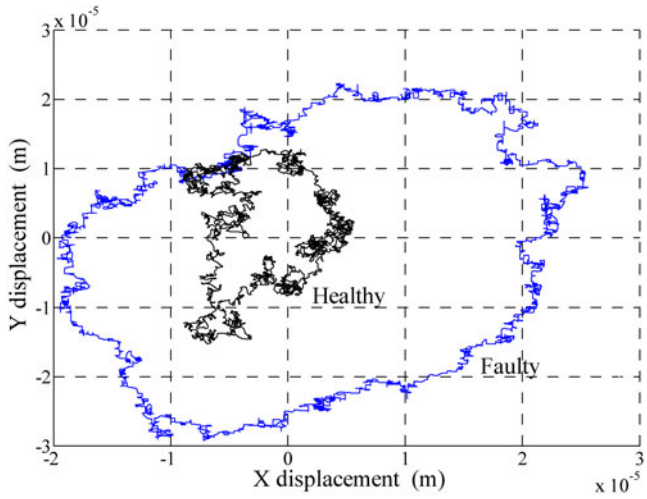

Fig. 14. 2-D trajectory of the shaft displacement in the $X-Y$ plane for a faulty and a healthy PMSM when running at 25 Hz.

In this measurement, the rotation frequency of the shaft was 25 Hz and the acquisition time was corresponding to two rotations of the shaft. The maximum amplitude variation of the difference signal is about 12 μm (± 6 μm) as presented in Fig. 11.

The difference is in full agreement with the ± 6 μm uncertainty calculated for the setup in Section II-C due to mechanical imperfections on the shaft surface. Thus, the self-mixing sensor has been shown to deliver valid results with a much cheaper sensor, which are only a bit more noisy than the reference ones.

IV. Results

Once the validity and accuracy of the technique have been analyzed in extent, we will present results for the 2-D trajectory of the lateral axis displacement using two SMLD arranged orthogonally (see Fig. 12). To observe the capabilities of the technique in NDT testing of PMSM motors, both a healthy PMSM and a faulty one have been measured using the same setup.

Fig. 13 depicts the 2-D displacement reconstruction of the shaft displacement in both motors. In the experiment, the SMS of two rotations acquired when the motors were running at 25 Hz is shown. Fig. 14 shows the 2-D trajectory of the displacement in polar coordinates. The shaft trajectory of the faulty PMSM may be seen to have a significantly higher amplitude and eccentricity.

V. Conclusion

A new compact, noncontact, and low-cost proximity probe based on SMI, and its associated procedure enabling runout measurement in PMSMs have been presented.

The proposed sensor is self-aligned and robust by nature, so the setup and procedure are very well suited to measurements in industrial conditions. Simple transition detection in self-mixing signal processing has been applied to get a basic resolution of $\lambda/2$ in the measurement. Details on the signal processing procedure were given. A new step, additional to the common self-mixing signal processing, has been implemented for misalignment correction. A new adaptive solution to speckle correction has been also applied in the measurements and has been described in detail.

A new configuration using two LDs in opposition was used as a procedure to estimate the uncertainty of the measurements, which was below ± 6 μm, due principally to shaft surface and shape imperfections.

In order to validate the measurement procedure, a commercial Polytec OFV-303 vibrometer was used simultaneously with an SMLD. Validation results show a maximum difference of ± 6 μm, equivalent to the uncertainty of the measurements. Results for NDT testing of PMSM motors have been shown, showing the 2-D difference in motor shaft displacements in a healthy and a faulty PMSM motor.

References

[1] M. J. DeBlock, B. M. Wood, and J. W. McDonnell, "Predicting shaft proximity probe track runout on API motors and generators," in *Proc. Pet. Chem. Ind. Tech. Conf.*, Calgary, Norway, 2007, pp. 1–8.

[2] J. Lin and M. Bissonnette, "A new capacitive proximity probe immune to electrical runout," in *Proc. Can. Mach. Vib. Assoc.*, Toronto, ON, Canada, 1997, pp. 1–5.

[3] J. Chass and F. Hills, "Linear variable differential transformer," U.S. Patent 3 546 648, Dec. 8, 1970.

[4] J. Shieh, J. E. Huber, N. A. Fleck, and M. F. Ashby, "The selection of sensors," *Prog. Mater. Sci.*, vol. 46, pp. 461–504, 2001.

[5] B. J. Halkon and S. J. Rothberg, "Rotor vibration measurements using laser doppler vibrometry: Essential post-processing for resolution of radial and Pitch/Yaw vibrations," *J. Vib. Acoust.*, vol. 128, no. 1, pp. 8–20, Feb. 2006.

[6] S. Royo, J. R. Ruiz, J. C. Urresty, and R. Atashkhooei, "Sistema y metodo de medida del desplazamiento transversal de un eje fisico giratorio," Patent P201 132 100, Dec. 23, 2011.

[7] S. Donati, "Developing self-mixing interferometry for instrumentation and measurements," *Laser Photon. Rev.*, vol. 6, pp. 393–417, 2012.

[8] S. Donati, *Electro-Optical Instrumentation—Sensing and Measuring With Laser*. Englewood Cliffs, NJ: Prentice-Hall, 2004, chs. 4 and 5.

[9] S. Ottonelli, M. Dabbicco, F. de Lucia, M. di Vietro, and G. Scamarcio, "Laser self mixing interferometry for mechatronics applications," *Sensors*, vol. 9, no. 5, pp. 3527–3548, May 2009.

[10] G. Guiliani, M. Norgia, S. Donati, and T. Bosch, "Laser diode self-mixing technique for sensing application," *J. Opt. A, Pure Appl. Opt.*, vol. 4, pp. S283–S294, 2002.

[11] N. Servagent, F. Gouaux, and T. Bosch, "Measurement of displacement using the self-mixing interference in a laser diode," *J. Opt.*, vol. 29, pp. 168–173, 1998.

[12] R. Lang and K. Kobayashi, "External optical feedback effects on semiconductor injection laser properties," *IEEE J. Quantum Electron.*, vol. QE-16, no. 3, pp. 347–355, Mar. 1980.

[13] W. M. Wang, K. T. V. Grattan, A. W. Palmer, and W. J. O. Boyle, "Self-mixing interference inside a single-mode diode laser for optical sensing applications," *J. Lightwave Technol.*, vol. 12, no. 9, pp. 1577–1587, Sep. 1994.

[14] S. Donati, G. Giuliani, and S. Merlo, "Laser diode feedback interferometer for measurement of displacements without ambiguity," *IEEE J. Quantum Electron.*, vol. 31, no. 1, pp. 113–119, Jan. 1995.

[15] C. Bes, G. Plantier, and T. Bosch, "Displacement measurements using a self-mixing laser diode under moderate feedback," *IEEE Trans. Instrum. Meas.*, vol. 55, no. 4, pp. 1101–1105, Jul. 2006.

[16] U. Zabit, F. Bony, T. Bosch, and A. D. Rakic, "A self-mixing displacement sensor with fringe-loss compensation for harmonic vibrations," *IEEE Photonics Technol. Lett.*, vol. 22, no. 6, pp. 410–412, Mar. 2010.

[17] U. Zabit, T. Bosch, and F. Bony, "Adaptive transition detection algorithm for a self-mixing displacement sensor," *IEEE Sensors J.*, vol. 9, no. 12, pp. 1879–1886, Dec. 2009.

[18] Y. Yu, J. Xi, and J. F. Chicharo, "Improving the performance in an optical feedback self-mixing interferometry system using digital signal preprocessing," in *Proc. IEEE Int. Symp. Intell. Signal Process.*, Oct. 3–5, 2007, pp. 1–6.

[19] J. Caum, J. Arasa, S. Royo, and M. Ares, "Design of adaptive digital filters for phase extraction in complex fringe patterns obtained using the Ronchi test," *J. Mod. Opt.*, vol. 59, no. 8, pp. 721–728, 2012.

[20] L. Wei, J. Chicharo, Y. Yu, and J. Xi, "Pre-processing of signals observed from laser diode self-mixing interferometries using neural networks," in *Proc. IEEE Int. Symp. Intell. Signal Process.*, Oct. 3–5, 2007, pp. 1–5.

[21] M. Norgia, S. Donati, and D. D'Alessandro, "Interferometric measurements of displacement on a diffusing target by a speckle tracking technique," *IEEE J. Quantum Electron.*, vol. 37, no. 6, pp. 800–806, Jun. 2001.

[22] U. Zabit, R. Atashkhooei, T. Bosch, S. Royo, F. Bony, and A. D. Rakic, "Adaptive self-mixing vibrometer based on a liquid lens," *Opt. Lett.*, vol. 35, no. 8, pp. 1278–1280, Apr. 2010.

[23] R. Atashkhooei, S. Royo, F. J. Azcona, and U. Zabit, "Analysis and control of speckle effects in self-mixing interferometry," in *Proc. IEEE Sens.*, Limerick, Ireland, Oct. 28–31, 2011, pp. 1390–1393.

[24] T. Bosch, C. Bes, L. Scalise, and G. Plantier, "Optical feedback interferometry," *Encycl. Sensors*, vol. 7, pp. 107–126, 2006.

Reza Atashkhooei was born in Khoy, Iran, in 1977. He received the B.Sc. degree in applied physics from Sharif University of Technology, Tehran, Iran, in 2001, and the M.Sc. degree in photonics from the Universitat Politècnica de Catalunya (UPC), Barcelona, Spain, in 2008. He is currently working toward the Ph.D. degree in optical engineering at the Centre for Sensors, Instruments and Systems Development (CD6 Research Center), UPC, Terrassa, Spain.

His current research interests include vibration and velocity measurements for industrial applications, signal processing, adaptive optics, and optical metrology.

Julio-César Urresty received M.S. degrees in electrical engineering and physics from the Universidad del Valle, Cali, Colombia, in 2006 and 2009, respectively. He is currently working toward the Ph.D degree in the Motion and Industrial Control Group at the Universitat Politècnica de Catalunya (UPC), Barcelona, Spain.

His research interests include signal processing methods, electric machines, variable-speed drive systems, and fault detection algorithms.

Santiago Royo received the M.Sc. degree in physics from the Universidad de Barcelona, Barcelona, Spain, and the Ph.D. degree in applied optics from the Universitat Politècnica de Catalunya (UPC), Barcelona, in1992 and 1999, respectively.

He is currently an Associate Professor with UPC and the Director of the Center for Sensors, Instruments, and Systems Development (CD6), a research and innovation center in optical engineering with a staff of 40 people in Terrassa, Spain. He is also a cofounder of one spin-off company of CD6, SnellOptics. As a Researcher, at CD6 he leads projects involving adaptive optics, 3-D imaging and optical metrology, in special in wavefront sensing and self-mixing interferometry. His research interests include adaptive optics, optical metrology, optical design and fabrication, and photometric testing.

Jordi-Roger Riba (M'09) received the M.S. degree in physics and the Ph.D. degree from the Universitat de Barcelona, Barcelona, Spain, in 1990 and 2000, respectively.

In 1992, he joined the Escola d'Enginyeria d'Igualada, Universitat Politècnica de Catalunya (UPC), Barcelona, Spain, as a Full-Time Lecturer, and he joined the Department of Electrical Engineering in 2001. He belongs to the Motion and Industrial Control Group, UPC. His research interests include electromagnetic device modeling, signal processing methods, electric machines, fault diagnosis in electric machines, and fault detection algorithms.

Luís Romeral (M'98) received the M.S. degree in electrical engineering and the Ph.D. degree from the Universitat Politècnica de Catalunya (UPC), Barcelona, Spain, in 1985 and 1995, respectively.

In 1988, he joined the Department of Electronic Engineering, UPC, where he is currently an Associate Professor and Director of the Motion and Industrial Control Group, whose major research activities concern induction and permanent magnet motor drives, enhanced efficiency drives, fault detection and diagnosis of electrical motor drives, and improvement of educational tools. He has developed and taught postgraduate courses on programmable logic controllers, electrical drives and motion control, and sensors and actuators.

Dr. Romeral is a member of the European Power Electronics and Drives Association and the International Federation of Automatic Control.